Proceedings of the
46th IEEE Conference on Decision and Control
New Orleans, LA, USA, Dec. 12-14, 2007

ThPI25.3

A Linear Time Varying Model Predictive Control Approach to the Integrated Vehicle Dynamics Control Problem in Autonomous Systems

P. Falcone*, M. Tufo*, F. Borrelli*, J. Asgari†, H. E. Tseng†

*Università del Sannio, Dipartimento di Ingegneria, 82100 Benevento, Italy

Email: {falcone,francesco.borrelli}@unisannio.it, manuela.tufo@libero.it

†Ford Research Laboratories, Dearborn, MI 48124, USA

Email: {jasgari,htseng,dhrovat}@ford.com

Abstract— A Model Predictive Control (MPC) approach for controlling active front steering, active braking and active differentials in an autonomous vehicle is presented. We formulate a predictive control problem in order to best follow a given path by controlling the front steering angle, brakes and traction at the four wheels independently, while fulfilling various physical and design constraints. At each time step a trajectory is assumed to be known over a finite horizon, and an MPC controller computes the system inputs in order to best follow the desired trajectory on slippery roads at a given entry speed. We start from the results presented in [1], [2] and formulate the MPC problem based on successive on-line linearization of the nonlinear vehicle model (LTV MPC).

Simulative results are presented, interpreted and compared against LTV MPC schemes which make use only of steering and/or braking.

I. INTRODUCTION

In Model Predictive Control (MPC) a model of the plant is used to *predict* the future evolution of the system [3]. Based on this prediction, at each time step t a performance index is optimized under operating constraints with respect to a sequence of future input moves in order to best follow a given trajectory. The first of such optimal moves is the *control* action applied to the plant at time t. At time $t+1$, a new optimization is solved over a shifted prediction horizon.

Parallel advances in theory and computing systems have enlarged the range of applications where real-time MPC can be applied [4], [5], [6], [7], [8]. Yet, for a wide class of "fast" applications the computational burden of Nonlinear MPC is still a serious barrier for its implementation. As an example, in [2] we have implemented a nonlinear MPC controller on a passenger vehicle for an Active Front Steering (AFS) system at 20 Hz, by using the state of the art of optimization solvers and rapid prototyping systems. We have shown that its real time execution is limited to low vehicle speed, because of its computational complexity.

Nevertheless, the capability of handling constraints in a systematic way makes MPC a very attractive control technique, especially for applications where the process is required to work *in wide operating regions* and close to the boundary of the set of admissible states and inputs. This has motivated the study of alternative MPC approaches, requiring the solution of simpler optimization problems in real-time. Most of these approaches are based on linear or piecewise-linear approximations of the nonlinear model of the plant.

The interested reader can refer to the paper [2] for a review of the existing approaches in literature.

In this paper we present an MPC controller based on successive on-line linearizations of the non-linear plant model. In the following we refer to this MPC scheme as Linear Time Varying Model Predictive Control (LTV MPC). We apply the LTV MPC to an autonomous vehicle dynamics control problem. In particular, we formulate an LTV MPC problem in order to best follow, at a reference speed, a given path by controlling active front steering, active braking and active differentials in an autonomous vehicle.

The work presented in this paper is the continuation of a study on the application of MPC techniques to vehicle dynamics control problems. In our first work [1] we investigated the potentiality of nonlinear MPC in solving an autonomous path following problem via AFS. The resulting Nonlinear MPC (NMPC) controller showed good performance but the computational complexity limited its implementation to low vehicle speed. In order to decrease the computational complexity, in [9], [2] we presented a LTV MPC approach to the path following via AFS problem. Experimental results [2] showed the capability of the controller to stabilize the vehicle up to 72 Kph in a double lane change manoeuvre on slippery (snow covered) surfaces.

In the present work we build on the aforementioned results and include additional control variables in the LTV MPC control algorithm. In particular we allow independent braking at the four wheels and active differentials (i.e., independent tractive torques at the four wheels).

Preliminary simulative results are presented and discussed. In particular, we highlight the simplicity of the proposed scheme in orchestrating nine different inputs with a minimal tuning effort. Simulation results up to 21 m/s on icy roads show the effectiveness of the proposed MPC formulation. We remark that the synthesis of any ad-hoc strategy which selects the wheels to brake or spin and the steering action depending on the driving condition, would result in a highly complex control design problem.

II. MODELING

This section describes the vehicle and tire model used for simulations and control design. The following nomenclature refers to the model depicted in Figure 1. For the sake of compact notation, next we use two subscript symbols to denote

variables related to the four wheels. In particular $\star \in \{f, r\}$ denote the front and rear axles, while $\bullet \in \{l, r\}$ denotes the left and right sides of the vehicle. For instance, the variable $(v)_{f,l}$ refers to the value of v at the front left wheel. We denote by $F_{l_{\star,\bullet}}$, $F_{c_{\star,\bullet}}$ the longitudinal (or "tractive") and lateral (or "cornering") tire forces, respectively. $F_{x_{\star,\bullet}}$ and $F_{y_{\star,\bullet}}$ are the components of the forces $F_{l_{\star,\bullet}}$ and $F_{c_{\star,\bullet}}$ along the longitudinal and lateral vehicle axes, respectively, $F_{z_{\star,\bullet}}$ the normal tire forces, X, Y the absolute car position in an inertial frame, a, b (distance of front and rear wheels from center of gravity) and c (distance of the vehicle longitudinal axis from the wheels) the car geometry, g the gravitational constant, m the car mass, I the car inertia, r the wheel radius, $s_{\star,\bullet}$ the slip ratios, $v_{l_{\star,\bullet}}$, $v_{c_{\star,\bullet}}$ the longitudinal and lateral wheel velocities, ψ the heading angle, $\dot{x}$ and $\dot{y}$ the vehicle longitudinal and lateral speed respectively, $\alpha_{\star,\bullet}$ the tire slip angles, $\delta_{\star}$ the wheel steering angles and $\mu_{\star,\bullet}$ the road friction coefficients at the four wheels.

A. Vehicle Model

We use a four wheels model to describe the dynamics of the car and assume constant normal tire load, i.e., $F_{z_{f,l}}, F_{z_{f,r}}, F_{z_{r,l}}, F_{z_{r,r}} =$ constant. Figure 1 depicts a diagram of the vehicle model, which has the following longitudinal, lateral and turning or yaw degrees of freedom (DOF)

$$m\ddot{x} = m\dot{y}\dot{\psi} + F_{x_{f,l}} + F_{x_{f,r}} + F_{x_{r,l}} + F_{x_{r,r}} \quad (1a)$$

$$m\ddot{y} = -m\dot{x}\dot{\psi} + F_{y_{f,l}} + F_{y_{f,r}} + F_{y_{r,l}} + F_{y_{r,r}}, \quad (1b)$$

$$I\ddot{\psi} = a\left(F_{y_{f,l}} + F_{y_{f,r}}\right) - b\left(F_{y_{r,l}} + F_{y_{r,r}}\right) \quad (1c)$$

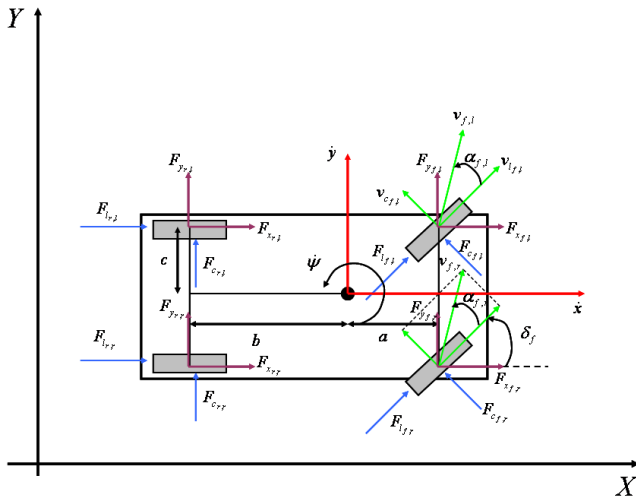$$+ c\left(-F_{x_{f,l}} + F_{x_{f,r}} - F_{x_{r,l}} + F_{x_{r,r}}\right). \quad (1d)$$

Fig. 1. The simplified vehicle dynamical model.

The vehicle's equations of motion in an absolute inertial frame are

$$\dot{Y} = \dot{x}\sin\psi + \dot{y}\cos\psi, \quad (2a)$$

$$\dot{X} = \dot{x}\cos\psi - \dot{y}\sin\psi. \quad (2b)$$

The lateral and longitudinal tire forces $F_{c_{\star,\bullet}}$ and $F_{l_{\star,\bullet}}$ lead to the components $F_{y_{\star,\bullet}}$ and $F_{x_{\star,\bullet}}$, along the lateral and longitudinal vehicle axes, respectively, computed as follows

$$F_{y_{\star,\bullet}} = F_{l_{\star,\bullet}}\sin\delta_{\star} + F_{c_{\star,\bullet}}\cos\delta_{\star}, \quad (3a)$$

$$F_{x_{\star,\bullet}} = F_{l_{\star,\bullet}}\cos\delta_{\star} - F_{c_{\star,\bullet}}\sin\delta_{\star}. \quad (3b)$$

Lateral and longitudinal tire forces for each tire are given by

$$F_{c_{\star,\bullet}} = f_c(\alpha_{\star,\bullet}, s_{\star,\bullet}, \mu_{\star,\bullet}, F_{z_{\star,\bullet}}), \quad (4a)$$

$$F_{l_{\star,\bullet}} = f_l(\alpha_{\star,\bullet}, s_{\star,\bullet}, \mu_{\star,\bullet}, F_{z_{\star,\bullet}}). \quad (4b)$$

The slip ratios $s_{\star,\bullet}$ are defined as

$$s_{\star,\bullet} = \begin{cases} \dfrac{r_w\omega_{\star,\bullet}}{v_{l_{\star,\bullet}}} - 1 & \text{if } v_{l_{\star,\bullet}} > r_w\omega_{\star,\bullet}, \ v_{l_{\star,\bullet}} \neq 0 \\ & \text{for braking} \\ 1 - \dfrac{v_{l_{\star,\bullet}}}{r_w\omega_{\star,\bullet}} & \text{if } v_{l_{\star,\bullet}} < r_w\omega_{\star,\bullet}, \ \omega_{\star,\bullet} \neq 0 \\ & \text{for driving,} \end{cases} \quad (5)$$

where $\omega_{\star,\bullet}$ are the wheels radius and angular speed respectively. The tire slip angles represent the angle between the wheel velocity and the direction of the wheel itself:

$$\alpha_{\star,\bullet} = \tan^{-1}\frac{v_{c_{\star,\bullet}}}{v_{l_{\star,\bullet}}}. \quad (6)$$

In equations (5) and (6), $v_{c_{\star,\bullet}}$ and $v_{l_{\star,\bullet}}$ are the lateral (or cornering) and longitudinal wheel velocities, respectively, which are expressed as

$$v_{c_{\star,\bullet}} = v_{y_{\star,\bullet}}\cos\delta_{\star} - v_{x_{\star,\bullet}}\sin\delta_{\star}, \quad (7a)$$

$$v_{l_{\star,\bullet}} = v_{y_{\star,\bullet}}\sin\delta_{\star} + v_{x_{\star,\bullet}}\cos\delta_{\star}, \quad (7b)$$

where

$$v_{y_{f,l}} = \dot{y} + a\dot{\psi} \quad v_{x_{f,l}} = \dot{x} - c\dot{\psi}, \quad (8a)$$

$$v_{y_{f,r}} = \dot{y} + a\dot{\psi} \quad v_{x_{f,r}} = \dot{x} + c\dot{\psi}, \quad (8b)$$

$$v_{y_{r,l}} = \dot{y} - b\dot{\psi} \quad v_{x_{r,l}} = \dot{x} - c\dot{\psi}, \quad (8c)$$

$$v_{y_{r,r}} = \dot{y} - b\dot{\psi} \quad v_{x_{r,r}} = \dot{x} + c\dot{\psi}. \quad (8d)$$

The tire vertical forces $F_{z_{\star,\bullet}}$ in (4) are computed as:

$$F_{z_{f,\bullet}} = \frac{bmg}{2(a+b)}, \quad F_{z_{r,\bullet}} = \frac{amg}{2(a+b)}. \quad (9)$$

Using the equations (1)-(9), the nonlinear vehicle dynamics can be described by the following compact differential equation:

$$\dot{\xi}(t) = f_{\mu(t)}(\xi(t), u(t)), \quad (10a)$$

$$\eta(t) = h(\xi(t)), \quad (10b)$$

where the state and input vectors are $\xi = [\dot{y}, \ \dot{x}, \ \psi, \ \dot{\psi}, \ Y, \ X]$ and $u = [\delta_f, \ s_{f,l}, \ s_{f,r}, \ s_{r,l}, \ s_{r,r}]$ respectively, $\mu = [\mu_{f,l}, \ \mu_{f,r}, \ \mu_{r,l}, \ \mu_{r,r}]$ and the output map is given as

$$h(\xi) = \begin{bmatrix} 0 & 1 & 0 & 0 & 0 & 0 \\ 0 & 0 & 1 & 0 & 0 & 0 \\ 0 & 0 & 0 & 1 & 0 & 0 \\ 0 & 0 & 0 & 0 & 1 & 0 \end{bmatrix} \xi. \quad (11)$$

Remark 1: Notice that model (10) has five inputs. In this preliminary work, we assume the existence of a low level braking and traction slip controller for each wheel and neglect its dynamics. The slip controllers regulate the current slip at each wheel to a negative (positive) desired slip through braking (traction) interventions at the wheels. Slip controllers could be avoided by a direct actuation of tractive and braking torques. In this case, the model (10) needs to be augmented with the dynamic model of the four wheels [10] and the MPC problem dimension increases.

B. Tire Model

The model for tire tractive and cornering forces (4) used in this paper is described by a Pacejka model [11]. This is a complex, semi-empirical model that takes into consideration the interaction between the tractive force and the cornering force in combined braking and steering. The longitudinal and cornering forces are assumed to depend on the normal force, tire slip angle, surface friction, and longitudinal slip.

III. LINEAR TIME VARYING (LTV) MODEL PREDICTIVE CONTROL

Consider the following discrete-time nonlinear system:

$$\xi(t+1) = f(\xi(t), u(t)), \tag{12}$$

where $\xi \in \mathbb{R}^n$ is the state vector, $u \in \mathbb{R}^m$ is the control input, $f(\cdot, \cdot) : \mathbb{R}^n \times \mathbb{R}^m \to \mathbb{R}^n$ is the state update function, and $f(0,0) = 0$, i.e., the origin of the state space is an equilibrium point. System (12) is subject to the following state and input constraints:

$$\xi(t) \in \mathcal{X}, \quad u(t) \in \mathcal{U}, \tag{13}$$

where $\mathcal{X} \in \mathbb{R}^n$ and $\mathcal{U} \in \mathbb{R}^m$ are polytopes.

A. LTV model approximation

Consider the state $\xi_0 \in \mathcal{X}$ and the input $u_0 \in \mathcal{U}$. Denote by $\hat{\xi}_0(k)$ for $k \geq 0$ the state trajectory obtained by applying the input sequence $u(k) = u_0$ for $k \geq 0$, to the system (12) with $\hat{\xi}_0(0) = \xi_0$, i.e.:

$$\begin{aligned} \hat{\xi}_0(k+1) &= f(\hat{\xi}_0(k), u(k)), \\ u(k) &= u_0, \\ \hat{\xi}_0(0) &= \xi_0. \end{aligned} \tag{14}$$

System (12) can be approximated by the following LTV system:

$$\delta\xi(k+1) = A_{k,0}\delta\xi(k) + B_{k,0}\delta u(k) \tag{15}$$

where $A_{k,0} \in \mathbb{R}^{n \times n}$ and $B_{k,0} \in \mathbb{R}^{n \times m}$ are defined as:

$$A_{k,0} = \left.\frac{\partial f}{\partial \xi}\right|_{\hat{\xi}_0(k), u_0}, \quad B_{k,0} = \left.\frac{\partial f}{\partial u}\right|_{\hat{\xi}_0(k), u_0}, \tag{16a}$$

$$\delta\xi(k) = \xi(k) - \hat{\xi}_0(k), \quad \delta u(k) = u(k) - u_0. \tag{16b}$$

The LTV system (16a) describes the deviations of the the nonlinear system (12) from the state trajectory $\hat{\xi}_0(t)$,

when an input sequence of constant amplitude u_0 is applied. Alternatively, the system (15) can be rewritten as

$$\xi(k+1) = A_{k,0}\xi(k) + B_{k,0}u(k) + d_{k,0}(k), \tag{17}$$

where $d_{k,0}(k) = \hat{\xi}_0(k+1) - A_{k,0}\hat{\xi}_0(k) - B_{k,0}u_0$ for $k \geq 0$.

Remark 2: System (15) and (17) are identical first order approximations of the system (12) around the nominal state trajectory $\hat{\xi}_0(k)$, $k \geq 0$. In (17) the nominal trajectory $\hat{\xi}_0(k)$ is hidden in the term $d_{k,0}(k)$.

In the next section we make use of the model (17) to formulate a model predictive control problem.

B. LTV MPC problem formulation

At each time t we consider the system

$$\xi(k+1) = A_{k,t}\xi(k) + B_{k,t}u(k) + d_{k,t}(k), \tag{18}$$

where the matrices $A_{k,t}$, $B_{k,t}$ and the vector $d_{k,t}$ are defined as in (16a)-(17), where the fixed index 0 has been replaced by t:

$$A_{k,t} = \left.\frac{\partial f}{\partial \xi}\right|_{\hat{\xi}_{k,t}, u_t}, \quad B_{k,t} = \left.\frac{\partial f}{\partial u}\right|_{\hat{\xi}_{k,t}, u_t}, \tag{19a}$$

$$d_{k,t} = \hat{\xi}_{k+1,t} - A_{k,t}\hat{\xi}_{k,t} - B_{k,t}u_t \tag{19b}$$

and:

$$\hat{\xi}_{k+1,t} = f(\hat{\xi}_{k,t}, u_t), \ k = t, \ldots, t+N-1 \tag{20a}$$

$$\hat{\xi}_{t,t} = \xi(t), \ u_t = u(t-1). \tag{20b}$$

The system (18) represents an LTV model approximation of the system (12) over a time horizon $k = t, \ldots, t+N-1$, where $N \in Z^+$.

Consider the cost function $V_N(\cdot, \cdot, \cdot) : \mathbb{R}^n \times \mathbb{R}^{Nm} \times \mathbb{R}^{Nn} \to \mathbb{R}^+$ defined as follows:

$$\begin{aligned} V_N(\xi(t), U(t), \Xi_{ref}(t)) &= \sum_{k=t+1}^{t+N-1} l(\xi(k), u(k), \xi_{ref}(t)) \\ &\quad + P(\xi(t+N), \xi_{ref}(t)), \end{aligned} \tag{21}$$

where $U(t) = [u(t), \ldots, u(t+N-1)]$ and $\Xi_{ref}(t) = [\xi_{ref}(t+1), \ldots, \xi_{ref}(t+N)]$ are a sequence of inputs and the reference state trajectory over the time horizon N, respectively, $\xi(k)$ for $k = t+1, \ldots, t+N$ is the state trajectory obtained by applying the control sequence $U(t)$ to the system (18), starting from the initial state $\xi(t)$, $l(\cdot, \cdot, \cdot) : \mathbb{R}^n \times \mathbb{R}^m \times \mathbb{R}^n \to \mathbb{R}^+$ is the stage cost and $P(\cdot, \cdot) : \mathbb{R}^n \times \mathbb{R}^n \to \mathbb{R}^+$ is the terminal cost.

At each sampling time t we consider the cost function

$V_N(\cdot, \cdot, \cdot)$ in (21) and the following problem:

$$\min_{U_t} \quad V_N(\xi_t, U_t, \Xi_{ref_t}) \tag{22a}$$

$$\text{s.t.} \quad \xi_{k+1,t} = A_{k,t}\xi_{k,t} + B_{k,t}u_{k,t} + d_{k,t}, \tag{22b}$$

$$\xi_{k,t} \in \mathcal{X} \tag{22c}$$
$$k = t+1, \ldots, t+N$$

$$u_{k,t} \in \mathcal{U} \tag{22d}$$
$$k = t, \ldots, t+N-1$$

$$\xi_{t+N,t} \in \mathcal{X}_f \tag{22e}$$

$$\xi_{t,t} = \xi(t). \tag{22f}$$

In (22), $U_t = [u_{t,t}, u_{t+1,t}, \ldots, u_{t+N-1,t}]$ and $\Xi_{ref_t} = [\xi_{ref_{t+1}}, \ldots, \xi_{ref_{t+N}}]$ are the optimization vector and reference state trajectory at time t, respectively, $\xi_{k,t}$ is the predicted state at time k, with $k = t+1, \ldots, t+N$, given the state measurement $\xi(t)$ at time t and obtained by starting from the state $\xi_{t,t} = \xi(t)$ and applying to system (22b) the input sequence $u_{t,t}, \ldots, u_{t+N-1,t}$.

Constraint (22e) is a final state constraint and $\mathcal{X}_f$ is a polytope. Once the solution $U_t^* = \left[u_{t,t}^*, \ldots, u_{t+N-1,t}^*\right]$ to problem (22) has been computed, the first sample of U_t^*

$$u(t, \xi(t)) = u_{t,t}^* \tag{23}$$

is applied to the plant (12).

We denote by

$$\xi_{cl}(t+1) = f_{cl}\left(t, \xi_{cl}(t)\right) \tag{24}$$

the system (12) with the control law (22)-(23).

Remark 3: The cost function (21) is convex, the constraints (22b)-(22e) are linear, therefore the optimization problem (22) is convex. It can be solved with efficient Linear Programming (LP) or Quadrating Programming (QP) solvers, if the functions $l(\xi, u)$ and $P(\xi)$ in (21) are convex piecewise-linear or quadratic, respectively.

Remark 4: Although the complexity of the optimization problem (22) greatly reduces compared to a Nonlinear MPC (NMPC) problem, where the nonlinear model (12) is used instead of the LTV model (18), (22b), we point out that the MPC formulation (22)-(23) requires N linearizations of the model (12). This setup time can be significant for high order models and long prediction horizons.

Assumption 1: In order to further reduce the computational complexity of the MPC scheme (22)-(23), in the following we will assume that $A_{k,t} = A_t$, $B_{k,t} = B_t$ for $k = t, \ldots, t+N-1$.

Remark 5: The stability of the closed-loop system (24) is not guaranteed. Preliminary stability results for the MPC control (22)-(23) have been presented in [12].

IV. ACTIVE STEERING, BRAKES AND DIFFERENTIAL VIA LTV MPC

The MPC control algorithm presented in Section III is used next in order to design an autonomous path following control algorithm, where the control inputs are the front steering angle and the slip ratios at the four wheels. The control objective is to follow a desire path, while keeping the longitudinal speed as close as possible to a given reference.

In order to obtain a finite dimensional optimal control problem we consider the model (10) and discretize the system dynamics with the Euler method, to obtain

$$\xi(k+1) = f_{\mu(k)}^{dt}(\xi(k), u(k)), \tag{25a}$$

$$u(k) = u(k-1) + \Delta u(k) \tag{25b}$$

$$\eta(k) = h(\xi(k)), \tag{25c}$$

where $u(k) = [\delta_f(k),\ s_{f,l}(k),\ s_{f,r}(k),\ s_{r,l}(k),\ s_{r,r}(k)]$, $\Delta u(k) = [\Delta\delta_f(k),\ \Delta s_{f,l}(k),\ \Delta s_{f,r}(k),\ \Delta s_{r,l}(k),\ \Delta s_{r,r}(k)]$ and $\mu(k) = [\mu_{f,l}(k),\ \mu_{f,r}(k),\ \mu_{r,l}(k),\ \mu_{r,r}(k)]$. In the rest of the paper we assume that

Assumption 2: The road friction coefficients at the four wheel are constants and all equal to μ_{snow}, i.e. $\mu_{f,l}(k) = \mu_{f,r}(k) = \mu_{r,l}(k) = \mu_{r,r}(k) = \mu_{snow}, \quad k \geq 0$.

We consider the following cost function:

$$V_{H_p}(\xi(t), \Delta\mathcal{U}_t) = \sum_{i=1}^{H_p} \left\|\hat{\eta}_{t+i,t} - \eta_{ref_{t+i,t}}\right\|_Q^2 +$$
$$\sum_{i=0}^{H_c-1} \|\Delta u_{t+i,t}\|_R^2 + \sum_{i=0}^{H_c-1} \|u_{t+i,t}\|_S^2 + \rho\epsilon \tag{26}$$

where, as in standard MPC notation [3], $\Delta\mathcal{U}_t = [\Delta u_{t,t}, \ldots, \Delta u_{t+H_c-1,t}]$ is the optimization vector at time t and $\hat{\eta}_{t+i,t}$ denotes the output vector predicted at time $t+i$ obtained by starting from the state $\xi_{t,t} = \xi(t)$ and applying to system (25) the input sequence $\Delta u_{t,t}, \ldots, \Delta u_{t+i,t}$. H_p and H_c denote the output prediction horizon and the control horizon, respectively. As in standard MPC schemes, we use $H_p > H_c$ and the control signal is assumed constant for all $H_c \leq t \leq H_p$, i.e., $\Delta u_{t+i,t} = 0 \ \forall i \geq H_c$. The reference signal η_{ref} represents the desired outputs, where $\eta = [\dot{x}, \psi, \dot{\psi}, Y]'$. Q, R and S are weighting matrices of appropriate dimensions. In (26) the first summand reflects the desired performance on target tracking, the second and the third summands are a measure of the steering and braking effort. The last term in (26) weights the slack variable ϵ associated to the soft constraints on tire slip angles, i.e., the tire slip angles are constrained within an interval centered in the origin. These constraints force the vehicle to operate within the linearity region of the tire characteristic (see [2] for further details).

The minimization of (26) subject to the model equation (25) is the base of the NLMPC scheme presented in [1], [2], [13].

V. SIMULATION RESULTS.

The control objective is to follow the path shown in Figure 2 as close as possible on a snow covered road ($\mu = 0.3$), while minimizing the deviation from the desired longitudinal speed ($\eta_{ref}(1) = \dot{x}_{ref}$ in (26)). The control inputs are the front tire steering angle and the slip ratios (positive and negative) at the four wheels.
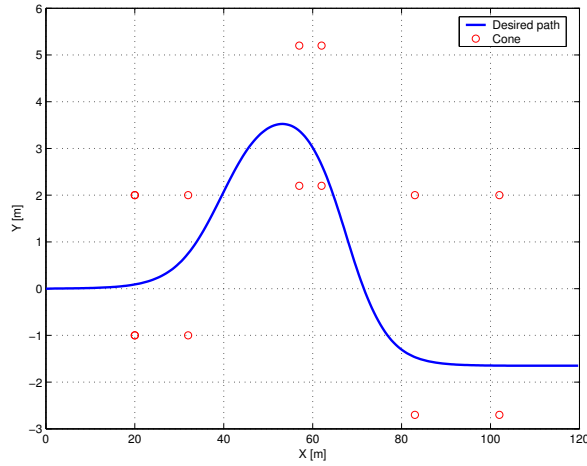
Fig. 2.   The reference path to be followed

Fig. 3.   Controller A. Yaw angle ψ (upper plot), yaw rate $\dot{\psi}$ (middle plot), lateral position Y (lower plot)

Fig. 4.   Controller A. Steering angle

Three tunings will be considered and the corresponding LTV MPC controllers denoted by Controller A, A1 and A2, respectively. The following parameters have been used for tuning of controller A:

- *sample time*: $T = 0.05$ sec;
- *constraints on inputs and input rates*: $\delta_{f,min}$=-10 deg, $\delta_{f,max}$=10 deg, $\Delta\delta_{f,min}$=-0.85 deg, $\Delta\delta_{f,max}$=0.85 deg. The upper and lower bounds on the four slip ratios are 2.7% and -2.7% respectively, the upper and lower bounds on the braking rate (i.e., Δs) are 10% and -10% respectively.
- *weights on tracking errors*: $Q_{\dot{x}} = 5 \cdot 10^{-4}$, $Q_\psi = 100$, $Q_{\dot{\psi}} = 1$, $Q_Y = 10$, $Q_{ij} = 0$ for $i \neq j$;
- *weights on input rates*: $R_{\delta_f} = 5 \cdot 10^3$, $R_{s_{f,l}} = 1 \cdot 10^{-3}$, $R_{s_{f,r}} = 1 \cdot 10^{-3}$, $R_{s_{r,l}} = 1 \cdot 10^{-3}$, $R_{s_{r,r}} = 1 \cdot 10^{-3}$, $R_{ij} = 0$ for $i \neq j$;
- *weights on input*: $S_{\delta_f} = 1 \cdot 10^{-7}$, $S_{s_{f,l}} = 1 \cdot 10^{-5}$, $S_{s_{f,r}} = 1 \cdot 10^{-5}$, $S_{s_{r,l}} = 1 \cdot 10^{-5}$, $S_{s_{r,r}} = 1 \cdot 10^{-5}$, $S_{ij} = 0$ for $i \neq j$;
- *horizons*: $H_p = 25$, $H_c = 10$.
- *constraints on the tire slip angles*: $\alpha_{f_{min}} = -3$ deg, $\alpha_{f_{max}} = 3$ deg, $\alpha_{r_{min}} = -3$ deg, $\alpha_{r_{max}} = 3$ deg.

Remark 6: Bounds on the slip ratio variations Δs have to be selected depending on the dynamics of the slip controller (see Remark 1). In particular upper bounds depend on the engine and driveline dynamics, while lower bound depend on the wheel dynamics and the braking system. As mentioned earlier, in this preliminary work we neglected the dynamics of the slip controller and thus select the bounds such that a fast variation of the slip ratios is allowed.

Figures 3-5 report the simulation results of the Controller A with $\dot{x}_{ref} = 21$m/s.

We observe that in Controller A a large deviation from the desired longitudinal speed is allowed by using a small weight $Q_{\dot{x}}$ and small weights on the braking and driving efforts at the four wheels. Moreover, high weights are used for the yaw, yaw rate and lateral position tracking errors. The longitudinal
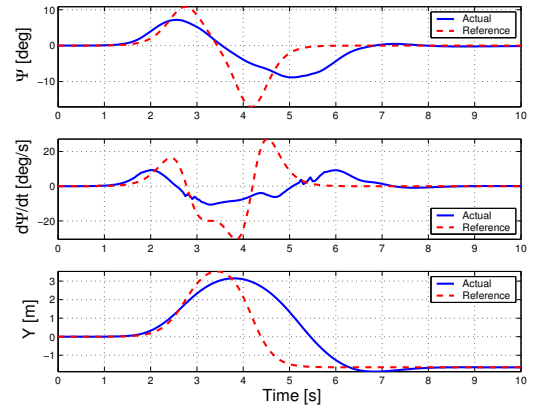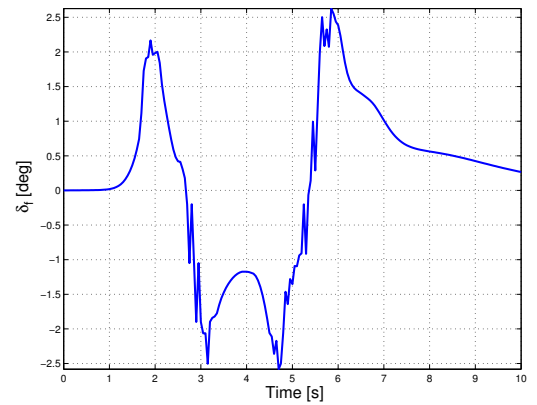
speed at the end of the double lane change is 19.8 m/s. As shown in Figure 3 the controller is able to stabilize the vehicle. We also observe that the controller is able to well coordinate the braking and the traction interventions at the four wheels, as well as the steering. Between 1 and 2 s the controller starts the manoeuvre by steering to the left to generate a positive yaw moment. During the same time interval, braking torques at both left-hand side wheels and traction torques at both right-hand side wheels are generated. This produces a positive yaw moment which helps the steering action. At 2 s the steering angle start to decrease, a traction torques is generated at both left-hand side wheels while the brakes are activated at both right-hand side wheels. The overall effect is a negative yaw moment. A similar behavior can be observed for the rest of the simulation.

Controller A is compared against *(i)* an LTV MPC controller without traction intervention (and same tuning of A) denoted by Controller A1 and presented in [14], *(ii)* an LTV MPC controller without traction and brake intervention (simple AFS controller) denoted by A2 and presented in [2], [13].

The Root Mean Squared tracking errors ($\bar{e}$.) and the final speed are reported in Table I. By comparing the RMS errors of controllers A and A1 in Table I, we observe that the
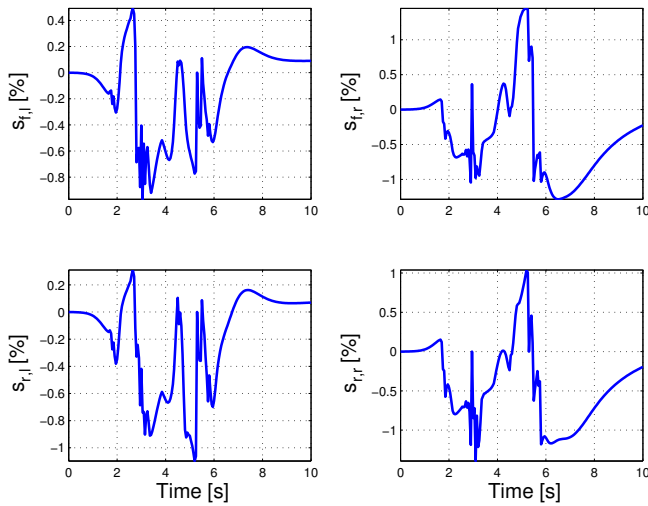
Fig. 5. Controller A. Slip ratios at the four wheels.

final longitudinal speed in controller A1 is significantly lower than controller A. The lower speed in controller A1 allows better tracking of the lateral position reference, although the performance in tracking of the yaw angle and the yaw rate references is worse. We finally observe that the tracking performance of controller A2 are definitely worse than controllers A1 and A2. In particular, by comparing controllers A and A2, we observe that controllers A has overall better tracking performances although the final longitudinal speeds in the two cases are almost the same.

	$\bar{e}_\Psi$	$\bar{e}_{\dot{\Psi}}$	$\bar{e}_Y$	$\dot{x}_{final}$
Controller A	$3.05 \cdot 10^{-2}$	$1.92 \cdot 10^{-1}$	14	19.8
Controller A1	$5.33 \cdot 10^{-2}$	$2.73 \cdot 10^{-1}$	11.49	16
Controller A2	$7.77 \cdot 10^{-2}$	$3.24 \cdot 10^{-1}$	26	20.6

TABLE I

RMS TRACKING ERROR FOR CONTROLLERS A AND B

VI. CONCLUSIONS

We presented an integrated steering, braking and active differential Model Predictive Control for autonomous path following. The presented approach has been tested in simulations with a double lane change manoeuvre on a snow covered road at high speed. The results showed an overall good tracking of the desired path. Moreover the comparison against a combined steering and braking MPC controller (i.e., negative slip ratios only), demonstrated that the controller can achieve better tracking performance without slowing down the vehicle excessively.

Future activities will aim to solve the same problem, by replacing the slip ratios with the braking and tractive torques. This would allow an easier implementation on a testing vehicle, since the low level slip controller (see Remark 1) would not be necessary anymore.

REFERENCES

[1] F. Borrelli, P. Falcone, T. Keviczky, J. Asgari, and D. Hrovat, "MPC-based approach to active steering for autonomous vehicle systems," *Int. J. Vehicle Autonomous Systems*, vol. 3, no. 2/3/4, pp. 265–291, 2005.

[2] P. Falcone, F. Borrelli, J. Asgari, H. E. Tseng, and D. Hrovat, "Predictive active steering control for autonomous vehicle systems," *IEEE Trans. on Control System Technology*, vol. 15, no. 3, 2007.

[3] D. Mayne, J. Rawlings, C. Rao, and P. Scokaert, "Constrained model predictive control: Stability and optimality," *Automatica*, vol. 36, no. 6, pp. 789–814, June 2000.

[4] F. Borrelli, A. Bemporad, M. Fodor, and D. Hrovat, "An MPC/hybrid system approach to traction control," *IEEE Trans. Control Systems Technology*, vol. 14, no. 3, pp. 541–552, May 2006.

[5] F. Borrelli, T. Keviczky, G. J. Balas, G. Stewart, K. Fregene, and D. Godbole, "Hybrid decentralized control of large scale systems," in *Hybrid Systems: Computation and Control*, ser. Lecture Notes in Computer Science. Springer Verlag, Mar. 2005.

[6] T. Keviczky and G. J. Balas, "Flight test of a receding horizon controller for autonomous uav guidance," in *Proc. American Contr. Conf.*, 2005.

[7] H. J. Ferrau, H. G. Bock, and M. Diehl, "An online active set strategy for fast parametric quadtratic programming in mpc applications," *IFAC Workshop on Nonlinear Model Predictive Control for Fast Systems, plenary talk*, 2006.

[8] V. M. Zavala, C. D. Laird, and L. T. Biegler, "Fast solvers and rigorous models: Can both be accomodated in nmpc?" *IFAC Workshop on Nonlinear Model Predictive Control for Fast Systems, plenary talk*, 2006.

[9] P. Falcone, F. Borrelli, J. Asgari, H. E. Tseng, and D. Hrovat, "A real-time model predictive control approach for autonomous active steering," in *Nonlinear Model Predictive Control for Fast Systems, Grenoble, France*, 2006.

[10] P. Falcone, F. Borrelli, H. E. Tseng, J. Asgari, and D. Hrovat, "Integrated braking and steering model predictive control approach in autonomous vehicles," *Fift IFAC Symposium on Advances of Automotive Control*, 2007.

[11] E. Bakker, L. Nyborg, and H. B. Pacejka, "Tyre modeling for use in vehicle dynamics studies," *SAE paper # 870421*, 1987.

[12] P. Falcone, F. Borrelli, J. Asgari, H. E. Tseng, and D. Hrovat, "Linear time varying model predictive control and its application to active steering systems: Stability analisys and experimental validation," *Accepted for publication on Journal of Robust and Nonlinear Control (*available at http://www.grace.ing.unisannio.it/home/pfalcone*)*, 2007.

[13] ——, "Predictive active steering control for autonomous vehicle systems," Universitá del Sannio. Dipartimento di Ingegneria., Tech. Rep., Jan. 2007, http://www.grace.ing.unisannio.it/publication/416.

[14] ——, "A model predictive control approach for combined braking and steering in autonomous vehicles," 15th *Mediterranean Conference on Control and Automation*, June 2007.